行政院國家科學委員會補助專題研究計畫成果報告

****
* 波導結構光電元件及相關介觀材料結構研究— *
* 子計畫三：半導體雷射與光放大器內非線性現象及其應用 *
****

計畫類別：整合型計畫

計畫編號：NSC 89-2218-E-002-097

執行期間：八十九年八月一日至九十年七月三十一日

計畫主持人：江衍偉，國立台灣大學電信工程學研究所

執行單位：國立台灣大學電信工程學研究所

中華民國九十年十月十九日

行政院國家科學委員會專題研究計畫成果報告

波導結構光電元件及相關介觀材料結構研究—
子計畫三：半導體雷射與光放大器內非線性現象及其應用

Nonlinear Phenomena in Semiconductor Lasers and Optical Amplifiers and Their Applications

計畫編號：NSC 89-2218-E-002-097
執行期間：八十九年八月一日至九十年七月三十一日
主持人：江衍偉、國立台灣大學電信工程學研究所
計畫參與人員：王志洋、陳祖傑、郭乃仁、林志南，國立台灣大學電信工程學研究所

摘要

我們藉一修正之時域行進波方法作數值模擬，探討了一全半導體光放大器非線性光環元件之交互開關的脈波操作特性。數值結果與吾人曾作過之實驗數據在趨勢上頗為吻合。
關鍵詞：數值模擬、光學開關、半導體光放大器

Abstract

The pulsed-signal operation of cross switching in an all-semiconductor-optical-amplifier nonlinear optical loop device is numerically investigated. Simulations were conducted using a modified time-domain traveling-wave method. Numerical results of simulation agreed well in physical trend with the reported experimental data.
Keywords: numerical simulation, optical switch, semiconductor optical amplifiers

All-optical nonlinear switching devices of the Sagnac interferometer type have received much attention due to their potential applications in high-speed communications and signal processing. Such a device basically consists of a loop structure for providing power-dependent gain/phase modulation and a 2x2 coupler for signal splitting/combination. When the input signal splits equally or unequally into two counter-propagating components in the loop, which contains a material of nonlinear optics effect, these two counter-propagating waves experience different gain/phase modulations. This difference then determines the distribution of signal power between the two output ports of the 2x2 coupler after the aforementioned two counter-propagating components recombine at the coupler. Because the cumulated difference in gain/phase modulation depends on the power level of input signal, the output power distribution of the device can be controlled by the input power. Such input power dependent behaviors can be used for self- and cross-switching operations in several applications.

The idea of this type of devices was first proposed implemented as a nonlinear optical loop mirror (NOLM), consisting of a fiber loop and a fiber coupler [1]. However, to increase the optical nonlinearity and to reduce the loop length, a semiconductor optical amplifier (SOA) was incorporated or even used to replace the fiber in the device. Recently, we have reported the fabrication and demonstration the CW- and pulsed-signal operations of an all-SOA nonlinear optical loop device [2]-[4]. The configuration of this device is similar to an NOLM, including an SOA loop and a multimode-interference waveguide amplifier (MMIWA) for closing the loop. From the experimental data, efficient all-optical switching was observed.

In this report, the pulsed-signal operation of cross switching in such an all-SOA nonlinear loop device is numerically

simulated. Device performances under various parameter conditions are investigated with relevant physical mechanisms interpreted. The numerical study was meant to simulate the experimental condition [4]. Here the asymmetric loop structure plays a crucial role. The power-dependent switching results from the combined effects of asymmetric gain/phase modulation in the loop and nonlinear coupling in the MMIWA.

Figure 1 shows the layout of the all-SOA nonlinear optical loop device. The device consists of several parts: the loop, the MMIWA, the input port and the output port. Note that the one-quarter and three-quarter sections of the loop are divided for different injection currents (I_4 and I_3, respectively). The injection currents for the regions of MMIWA and input/output portion are I_2 and I_1, respectively. All parts are made of ridge-loading waveguide SOAs. The loop with a ridge width of 4 μm (expected to form a single-lateral-mode waveguide) is connected to the MMIWA with a ridge of 8 μm wide where two modes can propagate. The input and output ports also have a ridge width of 4 μm. By injecting different currents, we can control the gain factors in different parts of the device.

In device operation, counter-propagating light waves exist simultaneously in the SOA. To simulate the colliding pulses in the MMIWA, we expand the TE-polarized electric field into two waveguide modes, each of which propagates in both forward and backward directions. In the loop region, only counter-propagating single-mode fields exist. In either the MMIWA or loop, we solve a set of differential equations for the forward- and backward-propagating wave fields as well as the rate equation for the carrier density. For simplicity, we have ignored any gain or loss in the input/output legs of the device. For numerical computation, the time-domain traveling-wave method [5] is employed to treat the counter-propagation problem. However, instead of using the first-order finite-difference approximation to the partial derivatives, we analytically solve the differential equations in each division segment along the waveguide axis to increase the numerical accuracy. The parameter values include the operating wavelength at 0.84 μm, the coupling length of the MMIWA at 1009.9 μm, the linewidth enhancement factor at 12, the carrier lifetime at 1 nsec, the internal loss coefficient of the MMIWA (loop) at $1000m^{-1}$ ($2000\ m^{-1}$), the length of the loop at 1.895 mm, the length of the MMIWA at 500 μm, and the effective waveguide area at 8 μm x 0.43 μm (4 μm x 0.43 μm) for the MMIWA (loop).

To investigate cross-switching phenomena, we conduct pump-probe simulation. Figure 2 shows the output energies of the probe pulse (from the output port, from the input port, and the sum from both ports) as functions of the time delay between the pump and probe. Here, the positive (negative) time delay means that the pump leads (lags) the probe. For comparison, we also compute the light transit times in the different device segments. The transit times in the MMIWA and one-quarter loop are about 5.67 ps and 5.39 ps, respectively. The input energy of the pump pulse is 0.05 pJ and that of the probe pulse is 0.002 pJ. Both the pump and probe have pulse width at 2 ps. The small-signal gain factors G_2, G_3 and G_4 are fixed at 4 dB, 5 dB and 35 dB, respectively. One can see that the curve of probe energy from the output port exhibits a hump around zero time delay and extends a long tail. This behavior can be interpreted qualitatively with the following mechanisms. When the probe leads significantly the pump, corresponding to a large negative time delay in Fig. 2 (a), the probe is not affected by the pump. This situation corresponds to the linear optics case, and a small amount of energy comes out from the output port. As the probe leads the pump by a small time interval, say, several picoseconds, the counterclockwise propagating probe pulse in the loop will experience gain saturation caused by the clockwise propagating pump pulse in the region including part of the high-gain one-quarter loop. Meanwhile, the clockwise propagating probe pulse in the

loop will experience gain saturation caused by the counterclockwise propagating pump pulse only in the low-gain loop region. The strong asymmetric gain/phase modulation experienced by the counter-propagating probe pulse then results in a significant variation of probe energy with respect to time delay. This explains the appearance of the peak of probe energy from the output port. Note that in this situation, the clockwise (counterclockwise) propagating pump pulse produces no effect on the clockwise (counterclockwise) propagating probe pulse because the pump lags behind the probe. When the pump leads the probe by a small time interval, corresponding to a small positive time delay in Fig. 2 (a), the gain in SOA is saturated by the pump pulse. Therefore, less gain/phase modulation for the probe results in smaller variation of the probe energy. As the pump leads the probe further, the probe pulse experiences the gradually recovered environment. No significant asymmetric gain/phase modulation is now expected for the probe. Figure 2 (b) shows the output probe energies after time delay beyond 50 ps. It can be seen that the probe energy gradually attains its unsaturated level at the time delay of the order of nanoseconds. This is consistent with the fact that the carrier lifetime here is assumed to be 1 ns. Note also that our simulated results agree in trend with the reported experimental data (see Fig. 15 in [4]).

To further understand the effect of asymmetric gain distribution in the loop, we vary the length of the high-gain (G_4) section with (G_3, G_2) fixed at (5 dB, 35 dB). In Fig. 3, three lengths of the high-gain section are used: one-eighth (dashed curve), one-quarter (solid curve), and three-eighths (dash-dotted curve) of the whole loop. For meaningful comparison, one end of the high-gain section is fixed at the midpoint of the loop. Other parameters remain the same as in Fig. 2, except that the input FWHM pulse width τ_p is reduced to 1 ps. In Fig. 3, one can see that as the high-gain section becomes longer, cross-switching occurs earlier. This trend can be explained with the aforementioned physical mechanisms. As the probe pulse leads the pump pulse by a few picoseconds, the counterclockwise propagating probe pulse in the loop will experience gain saturation caused by the clockwise propagating pump pulse in the region involving the high-gain section. Also, the clockwise propagating probe pulse in the loop will experience gain saturation caused by the counterclockwise propagating pump pulse only in the low-gain loop section. The strong asymmetric gain/phase modulation experienced by the counter-propagating probe signal results in a fast variation of the probe energy. Now, if the length of the high-gain section increases, larger time delay between pump and probe pulses is allowed to evoke this phenomenon, and the curve of the output probe energy shifts toward the negative side of time delay accordingly. Therefore, Fig. 3 again verifies that the asymmetric gain distribution along the loop is important for efficient pulsed-signal operation.

In summary, the pulsed-signal operation of cross switching in an all-semiconductor-optical-amplifier loop device has been numerically demonstrated, showing efficient power-dependent switching effect. Besides the nonlinear coupling in the MMIWA and the lateral field redistribution and amplification in the loop, the asymmetric gain distribution along the loop is crucial for efficient pulsed-signal operation.

References

1. N. J. Doran and D. Wood, "Nonlinear-optical loop mirror," Opt. Lett., Vol. 13, pp. 56-58, 1988.
2. J. H. Lee, D. A. Wang, H. J. Chiang, D. W. Huang, S. Gurtler, C. C. Yang, Y. W. Kiang, B. C. Chen, M. C. Shih and T. J. Chuang, "Nonlinear switching in an all-semiconductor-optical-amplifier loop device," IEEE Photon. Technol. Lett., Vol. 11, pp. 236-238, 1999.
3. J. H. Lee, D. A. Wang, Y. W. Kiang, H. J. Chiang and C. C. Yang, "Nonlinear switching behaviors in a compact all-semiconductor optical-amplifier Sagnac

interferometer device," IEEE J. Quantum Electron., Vol. 35, pp. 1469-1477, 1999.
4. J. H. Lee, J. Y. Wang, C. C. Yang and Y. W. Kiang, "All-optical switching behaviors in an all-semiconductor nonlinear loop device," J. Opt. Soc. Am. B., Vol. 18, pp. 1334-1341, 2001.
5. L. M. Zhang, S. F. Yu, M. C. Nowel, D. D. Marcenac, J. E. Carroll, and R. G. S. Plumb, "Dynamic analysis of radiation and side-mode suppression in a second-order DFB laser using time-domain large-signal traveling wave model," IEEE J. Quantum Electron., Vol. 30, pp. 1389-1395, 1994.

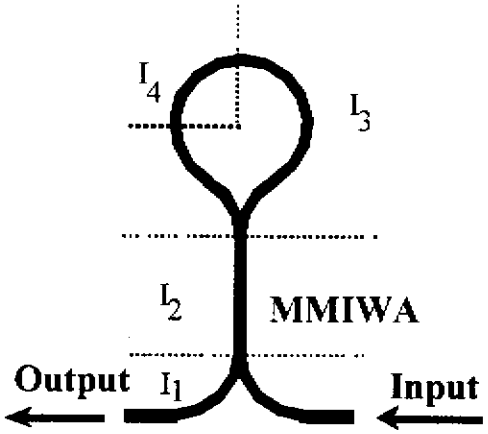

Fig. 1 Layout of the all-semiconductor nonlinear loop device.

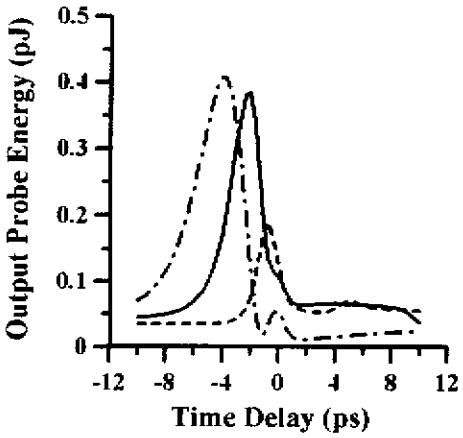

Fig. 3 Output energy of the probe pulse (from the output port) versus time delay between pump and probe for different lengths of the high-gain (G_4) section of the loop. Three lengths of the high-gain section are used: one-eighth (dashed curve), one-quarter (solid curve), and three-eighths (dash-dotted curve) of the whole loop.

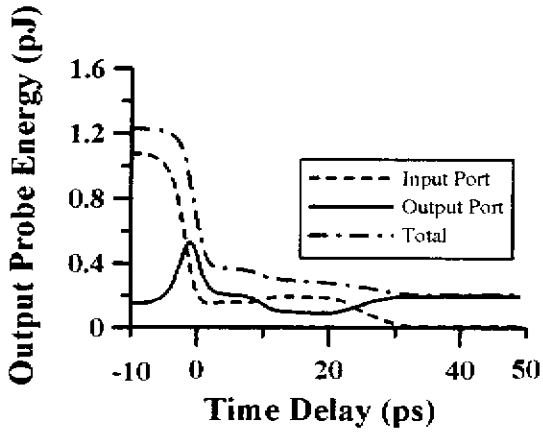

(a)

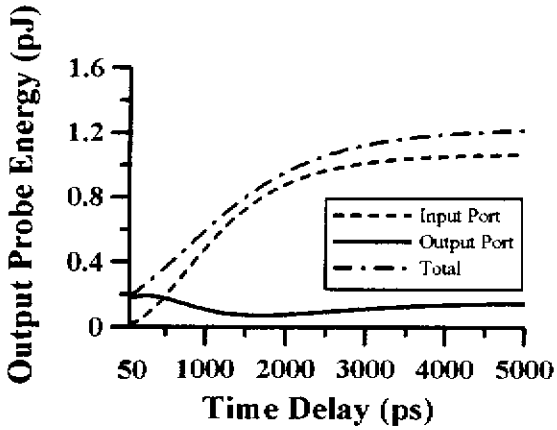

(b)

Fig. 2 Output energies of the probe pulse (from the output port, input port, and their sum) as functions of time delay between pump and probe.